

TISSUE ENGINEERING APPLICATIONS OF POLYHYDROXYBUTYRATE

A Report

Presented to the Faculty of the Graduate School

of Cornell University

In Partial Fulfillment of the Requirements for the Degree of

Master of Engineering

by

Esha Mathew

August 2008

© 2008 Esha Mathew

## ABSTRACT

Polyhydroxybutyrate (PHB) is an aliphatic biopolyester synthesized as a carbon and energy source by certain microorganisms with the enzyme PHA synthase. Due to its biocompatibility, PHB has been widely evaluated for a wide variety of tissue engineering applications. A method to extract the active PHA synthase enzyme and pattern it on various solid surfaces was established. Upon application of the enzyme's substrate, PHB polymer granules were formed via enzyme-linked surface initiated polymerization, providing an *in situ* organic coating on a variety of inorganic solid surfaces. In this work, the suitability of this enzyme-linked surface initiated polymerization (ESIP) of PHB was evaluated in two applications: as a platform for the propagation of embryonic stem cells, and as a noninvasive means for bone repair.

## BIOGRAPHICAL SKETCH

Esha entered Cornell as a freshman in 2003 and received her Bachelor of Science in Biological Engineering in 2007. She attended the Cornell graduate school the following year and completed her Master of Engineering in Biological Engineering in 2008.

To Mom, Appa, and Divij.

## ACKNOWLEDGMENTS

A big thanks to Dr. Carl Batt for giving me wonderful research opportunities in his lab, and to Dr. Dan Aneshansley for taking me on as an advisee. I also want to thank all the members of Battlab for their help, advice, and making the lab such a fun place to work. I also want to thank Dr. Nuttawee Niamsiri for being an incredible research mentor. Her guidance and infinite patience as I learned the ins and outs of lab work have made me a better student and researcher. Finally, I would like to thank my family for all their love and support.

## TABLE OF CONTENTS

|                                |      |
|--------------------------------|------|
| Biographical Sketch . . . . .  | iii  |
| Dedication . . . . .           | iv   |
| Acknowledgements . . . . .     |      |
| Table of Contents . . . . .    | vi   |
| List of Figures . . . . .      | viii |
| List of Symbols . . . . .      | ix   |
| List of Abbreviations. . . . . | x    |

### **1 –Overview**

|  |   |
|--|---|
| 1.1 – Introduction . . . . .               | 1 |
| 1.2 –Polyhydroxyalkanoates. . . . .        | 1 |
| 1.3 – Stem Cells.....                      | 2 |
| 1.4 – Biomaterials and Stem Cells. . . . . | 2 |
| 1.5 – Conclusion . . . . .                 | 2 |
| 1.6 – References.....                      | 2 |

### **2 – Murine Embryonic Stem Cell Biocompatibility Study on Two Dimensional Solid Surfaces Modified with Polyhydroxybutyrate via Enzymatic Surface-Initiated Polymerization**

|   |   |
|---|---|
| 2.1 – Abstract.....                         | 5 |
| 2.2 –Introduction.....                      | 9 |
| 2.3 –Materials and Methods.....             | 9 |
| 2.4 – Results and Discussion.. . . .        | 9 |
| 2.5 – Conclusions and Future Work . . . . . | 9 |
| 2.6 – References.....                       | 9 |

### **3 – Evaluation of Iron Oxide Nanoparticle-PHA synthase Conjugates for Application as a Noninvasive Means of Bone Repair**

|   |    |
|---|----|
| 3.1 – Abstract.....                     | 21 |
| 3.2 – Introduction.....                 | 23 |
| 3.3 –Materials and Methods.....         | 25 |
| 3.4 – Conclusions and Future Work. .... | 26 |
| 3.5 – References.....                   | 27 |

### **Appendices**



## LIST OF FIGURES

|   |    |
|---|----|
| 1.2 General Structure of Polyhydroxyalkanoates                    | 3  |
| 1.3 ES cell in vivo   | 7  |
| 2.4 AFM Analysis of ESIP PHB                                      | 20 |
| 2.4 Summary of MTT assays   | 21 |
| 2.4 Calculation of cell proliferation of test surfaces            | 21 |
| 2.4 Immunostaining results for mES cells on test surfaces         | 22 |
| 3.2 Overview of proposed mechanism for NP-PHA synthase conjugates | 28 |
| 3.4 Fluorescent images of PHB polymerization                      | 33 |
| 3.4 TEM analysis of NP-PHA synthase conjugates                    | 33 |
| 3.4 Magnetic nanoparticles dispersed throughout an agarose gel    | 34 |
| 3.4 NP-PHA synthase conjugates in small bone sections             | 35 |
| 3.4 MTT Assay Summary   | 36 |
| 3.4 ALP Assay Summary   | 37 |

## LIST OF ABBREVIATIONS

|          |  |
|----------|--|
| ALP      | alkaline phosphatase   |
| BSA      | bovine serum albumin   |
| ESIP     | enzymatic surface initiated polymerization                   |
| mES cell | murine embryonic stem cell                                   |
| MTT      | 3-(4,5-Dimethylthiazol-2-yl)-2,5-diphenyltetrazolium bromide |
| MNP      | magnetic nanoparticle  |
| PBS      | phosphate buffered saline                                    |
| PHA      | polyhydroxyalkanoate   |
| PHB      | polyhydroxybutyrate  |
| SDS      | sodium dodecyl sulfate                                       |
| TEM      | tunneling electron microscope                                |

## LIST OF SYMBOLS

|               |                   |
|---------------|-------------------|
| Au            | gold              |
| C             | Celsius           |
| DI            | deionized (water) |
| mM            | millimolar        |
| nm            | nanometer         |
| $\mu\text{L}$ | microliter        |

# **CHAPTER 1**

## **OVERVIEW**

## 1.1 Introduction

Tissue engineering is a broad term that encompasses applications relating to replacement of lost or damaged tissue. One commonly utilized definition by Langer and Vacanti states it as "an interdisciplinary field that applies the principles of engineering and life sciences toward the development of biological substitutes that restore, maintain, or improve tissue function or a whole organ." Tissue engineering is further subdivided into three categories: drug delivery, scaffold mediated therapy, and cell therapy (Langer and Vacanti 1996).

The key characteristic of tissue engineering is its focus on restoring lost functionality. Palliatives and supplements, such as ibuprofen for osteoarthritis and insulin for diabetes, merely relieve symptoms but do not address the underlying cause of illness and do not restore functionality. Transplants may restore functionality, but donor tissues and organs are limited and the patient demand is high. The development of engineering strategies to correct malfunctioning tissues in a reproducible manner attempts to overcome the shortcomings of conventional palliative or transplant methods. One area of development that has allowed major advances in tissue engineering is enabling biomaterials. Enabling biomaterials mimic aspects of the native conditions found in the extracellular matrix, allowing for control of cell attachment and behavior. One such biomaterial of particular focus in the laboratory of Dr. Carl Batt is the polyhydroxyalkanoate (PHA) family.

In Batt's lab, a technique was developed to isolate the enzyme responsible for the polymerization of polyhydroxybutyrate, a member of the PHA family, and tether it to a surface. Addition of the substrate allowed for the synthesis of PHB granules *in situ*. This system can be tailored to

attach the enzyme to a variety of solid surfaces, including gold and iron oxide nanoparticles. In this work, the application of this enzyme-linked surface initiated polymerization (ESIP) of PHB was investigated in regards to biomaterial-based control of cell behavior. A brief overview on the various elements of this study follows.

## 1.2 Polyhydroxyalkanoates

Polyhydroxyalkanoates (PHAs) have been widely evaluated for use in tissue engineering applications. PHAs are aliphatic polyesters produced in certain microorganisms by enzymes termed PHA synthases, which polymerize monomers of hydroxy fatty acids (R-hydroxyacyl-CoA) into larger intracellular granules (Jendrossek 2001). This polymerization is concomitant with the release of CoA.

The diameter of these water-insoluble granules ranges from 0.2-0.5  $\mu\text{m}$ , and the molecular weights range from  $2 \times 10^5$  to  $3 \times 10^6$  Da. The exact value is dependant on the specific organism, environmental factors, and the enzyme itself (Matsumoto et. al., 2006,). The physiological role of these biopolyesters is as a carbon and energy source for the organism, so PHA synthesis occurs in the presence of excess carbon but limited nutrients such as oxygen and phosphate (Shlegel et. al. 1961). The general structure of PHA is as shown in Figure 1.

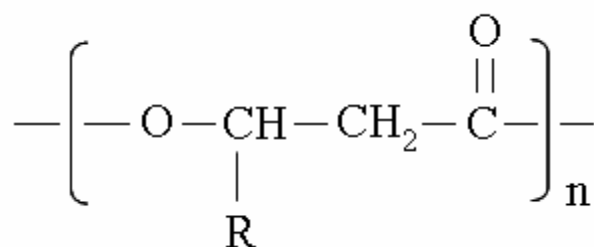


**Figure 1:** General structure of polyhydroxyalkanoates (PHAs)

There are many variants of PHA, which range from crystalline to amorphous. The properties of the polymer are dictated by either the structure and sequence of the monomer, or by the type of side group, R. Crystalline forms of PHA have short chain lengths of hydroxy acid monomers at three to five carbon atoms. The amorphous forms generally have medium chain length hydroxy acid monomers at six to fourteen carbon atoms (Kim and Lenz 2001, Rehm and Steinbüchel 2001). The side group moiety can include carboxyl, halogens, epoxy, hydroxyl, cyanophenoxy, thiophenoxy, methylester, and nitrophenoxy groups, and can influence many of its properties including melting point and crystallinity. The most ubiquitous form of PHA is poly (3-hydroxybutyrate), abbreviated as PHB. This subset of the PHA family has a methyl moiety as its side group. PHB is characterized by a high percentage crystallinity, and is thus stiff, brittle, and has a high melting temperature. ESIP-PHB however, does not have the same properties as its compression-molded counterpart.

#### *Enzyme-Linked Surface Initiated Polymerization*

The ability to grow and pattern inorganic and/or solid surfaces with organic coatings is useful for applications in tissue engineering and biosensors. There are three general methods for the modification of solid surfaces. The first, spin casting, involves deposition of an organic substance via adsorption, which is reversible under certain conditions. The second method is grafting, and it entails attachment of an organic polymer to a surface using chemical modification, such as an amide or ester linkage. Both spin coating and grafting are hampered by the potential for desorption and limitation to low density polymer structures respectively (Dyer 2003).

The third method, surface-initiated polymerization (SIP), overcomes the issues seen with the former two methods and produces films that are denser, robust, and compatible with micro and nanolithography processes. In SIP, the polymerization initiator is linked to the surface. Thus, the ensuing polymer chain is then grown out and away from the initiator, but remains tethered to the surface (Kim et. al. 2000, Dyer 2003). Due to its superior surface modification ability, SIP has been extensively investigated. In our laboratory, a technique has been developed to harness the action of the PHA synthases to form polymeric structures from the bottom-up on solid surfaces (Kim et. al. 2004). Thus, utilization of a biologically active molecule to catalyze microstructures is termed ‘bionanofabrication’ (Delamarre et. al. 2006).

Our focus is the fact that bionanofabrication of PHB on solid surfaces allows the engineering of cell-surface interaction for control of cell behavior. Recent work in our lab has shown site-specific attachment of PHA synthase on patterned surfaces. Addition of the enzyme substrate, allowed for the growth of spatially ordered PHB structures *in situ*. Biocompatibility studies with fibroblasts showed preferential cellular adhesion on the PHB patterned surfaces. This ability to control cell adhesion, in a specific manner on surfaces, is important for use in tissue engineering and cell-based biosensor technology (Niamsiri 2007).

It would be useful to extend these studies to the control of murine embryonic stem cell behavior. Currently, there is a great deal of research on the use of biomaterials to control and direct stem cell behavior, with the hope of one day implementing them in a clinical setting.



## 1.3 Stem Cells

### *Introduction*

Stem cells are undifferentiated cells that possess the ability to self-renew for an extended period of time, and differentiate into more specialized phenotypes. The two major types of mammalian stem cells are adult and embryonic stem cells. Adult stem cells exist in the fully developed organism and do not exhibit total plasticity, thus termed multipotent. These cells can be found at certain points in the body, called ‘niches’, which can be found in the blood, bone marrow and brain. In such particular locations, these adult stem cells are restricted in their lineage potential. For instance, a stem cell found in the brain will terminally differentiate into either neurons or glia. Although some studies have found methods of transdifferentiation, work in this area is still in progress. Embryonic stem cells, in contrast, are pluripotent. They have the ability to terminally differentiate into any cells derived from the three embryonic germ layers – endoderm, ectoderm, and mesoderm. Both types of stem cells can be used as tools for understanding the processes behind mammalian tissue and organ development. They also hold promise in therapeutic applications, especially where standard treatments have proven less effective.

### *Embryonic Stem Cells*

Embryonic stem cells are obtained from the inner cell mass of the blastocyst. After fertilization of the egg, the ensuing zygote undergoes a series of precisely tuned divisions. At the blastocyst stage, the developing embryo consists of a hollow ball filled with an inner cell mass, as shown in figure 2. Embryonic stem cells are derived from this inner cell mass.

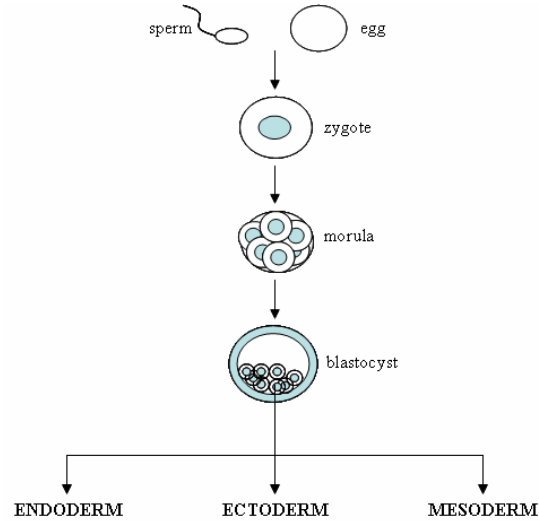


**Figure 2:** Upon fertilization, the ensuing zygote undergoes a series of divisions to reach the blastocyst stage. The inner cell mass is what embryonic stem cells comprise, and can derive cells from the three germ layers, as well as germ cells. Adapted from Wobus and Boehler 2005.

### *Murine Embryonic Stem Cells*

Unlike their human counterparts, murine embryonic stem cells (mES cells) are better characterized, probably due to the lack of ethical issues surrounding their extraction. These cells exhibit certain properties, including pluripotency, indefinite maintenance, stability of karyotype, and the display of certain unique markers on the cell surface, such as Oct-4 (Wobus and Boeheler 2005).

*In vitro* culture of mESCs is usually performed as a co-culture with murine embryonic fibroblast cells (MEFs), also termed a ‘feeder layer’. The reason for the feeder layer is due to the fact the MEFs secrete leukemia inhibitory factor (LIF), a cytokine necessary to maintain murine stem cell self-renewal and their undifferentiated state. LIF initiates the JAK/STAT pathway upon binding the proper receptor. This binding causes subsequent intracellular conformational

changes to the cytoplasmic face of the receptor, which in turn activates receptors associated with the Janus Kinase (JAK) family. Various other molecules are then phosphorylated (activated) leading to the activation of signal transducers and activators of transcription (STATs), which translocate to the nucleus and activate transcription of target genes (Kisseleva et. al. 2002). It is important to note that while involved in self-renewal of mES cells, the LIF/STAT pathway in human ES cells has not been elucidated (Sato et. al. 2005).

#### *Differentiating Murine Embryonic Stem Cells*

Differentiating mES cells *in vitro* can be performed several ways. The common trend in all methods is initial formation of cellular aggregates termed embryonic bodies (EBs) in a form of suspension culture. Upon formation of EBs, the cells will then differentiate spontaneously into a variety of cell types. Co-culture with a differentiated cell type and/or addition of growth factors or cytokines to the media will direct mESC differentiation to the desired subtype. However, the differentiated population is not homogenous, and separation methods to extract the cells desired are required (Xu et. al. 2008).

### **1.4 Biomaterials and Stem Cells**

There has been a great deal of progress in basic biology research to elucidate the molecular mechanisms governing stem cell characteristics. With this progress, the actual application of these cells in a clinical setting draws nearer. Concurrent research has been underway to create and evaluate a broad spectrum of biomaterials for their suitability in modifying ES cell behavior. One common bottleneck that occurs with the use of ES cells in tissue engineering is an inadequate population of cells. Commercially available products such as Matrigel have proved

promising for the expansion of undifferentiated cells. However, the animal origin of these products makes them unfavorable in the long run due to batch variability and immunogenic factors (Chai and Leong 2007). Other materials, such as silk and various treated polyesters have been evaluated, not just for the expansion of ES cells but also for the formation of three dimensional scaffolds for tissue and organ reconstruction (Wang et. al. 2006, Harrison et. al. 2004).

### **1.5 Conclusion**

It is believed that ESIP-PHB can be tailored for use in a variety of applications (Niamsiri et. al. 2007). Solid surfaces modified with ESIP-PHB have shown improved cellular proliferation on modified surfaces, and even preferential attachment on surfaces patterned with PHB. The ability to grow a PHB *in situ* lends itself well to events where provision of a matrix allows cell to migration and synthesis of extracellular matrix molecules to repair a defect. These applications were investigated further, by a) analyzing ESIP-PHB suitability to the culture of undifferentiated ES cells and b) evaluating the use of magnetic nanoparticle-PHA synthase conjugates for bone repair.

### **1.6 References**

- Bain, Gerard, Daniel Kitchens, Min Yao, James E. Huettner, and David Gottlieb. "Embryonic Stem Cells Express Neuronal Properties in Vitro." Developmental Biology 168 (1995): 342-357.
- Chai, Chou, and Kam W. Leong. "Biomaterials Approach to Expand and Direct Differentiation of Stem Cells." Molecular Therapy 15 (2007): 467-480.
- Delamarre, Soazig C., Nutawee Niamsiri, and Carl Batt. Bionanofabrication: a Tool for Creating Unique Structures Through in Vitro Polymer Synthesis. Microbial Bionanotechnology:

Biological Self-Assembly Systems and Biopolymer Based Nanostructures. Norwich, U.K.: Horizon Scientific P, 2006. 35-64.

Dyer, Daniel. "Patterning of Gold Substrates by Surface-Initiated Polymerization." Advanced Functional Materials 13 (2003): 667-670.

Harrison, J, S Pattanawong, J Forsythe, K Gross, D Nisbet, H Beh, T Scott, A Trounson, and R Mollard. "Colonization and Maintenance of Murine Embryonic Stem Cells on Poly( $\alpha$ -Hydroxy Esters)." Biomaterials 25 (2004): 4963-4970.

Jendrossek, D. "Microbial Degradation of Biopolyesters." Advances in Biochemical Engineering and Biotechnology 71 (2001): 294-325.

Kim, Jong-Bum, Merlin L. Bruening, and Gregory L. Baker. "Surface-Initiated Atom Transfer Radical Polymerization on Gold At Ambient Temperature." J. Am. Chem. Soc. 122 (2000): 7616-7617.

Kim, Young Baek, and Robert W. Lenz. "Polyesters From Microorganisms." Biopolyesters 71 (2001): 51-79.

Kim, Young-Rok, Hyun-Jong Paik, Christopher K. Ober, Geoffrey W. Coates, and Carl A. Batt. "Enzymatic Surface-Initiated Polymerization: a Novel Approach for the in Situ Solid-Phase Synthesis of Biocompatible Polymer Poly(3-Hydroxybutyrate)." Biomacromolecules 5 (2004): 889-894.

Kisseleva, T., S. Bhattacharya, J. Braunstein, and C W. Schindler. "Signaling Through the JAK/STAT Pathway, Recent Advances and Future Challenges." Gene 285 (2002): 1-24.

Langer, R, and JP Vacanti. "Tissue Engineering." Science 260 (1993): 920-926.

Matsumoto, Ken'ichiro, Yuko Arai, Rina Nagao, Takaaki Murata, Kazuma Takase, Hideo Nakashita, Seiichi Taguchi, Hiroaki Shimada, and Yoshiharu Doi. "Synthesis of Short-Chain-Length/Medium-Chain-Length Polyhydroxyalkanoate (PHA) Copolymers in Peroxisome of the Transgenic Arabidopsis Thaliana Harboring the PHA Synthase Gene From Pseudomonas Sp. 61-3." Journal of Polymers and the Environment 14 (2006): 369-374.

Muñoz-Sanjuán, Ignacio, and Ali H. Brivanlou. "Neural Induction, the Default Model and Embryonic Stem Cells." Nature Neuroscience 3 (2002): 271-280.

Niamsiri, Nuttawee, Magnus Bergkvist, Soazig C. Delamarre, Nathan C. Cady, Geoffrey W. Coates, Christopher K. Ober, and Carl A. Batt. "Insight in the Role of Bovine Serum Albumin for Promoting the in Situ Surface Growth of Polyhydroxybutyrate (PHB) on Patterned Surfaces Via Enzymatic Surface-Initiated Polymerization." Colloids and Surfaces B: Biointerfaces. 60 (2007): 68-79.

Rehm, B, and A Steinbüchel. "PHA Synthases: the Key Enzymes of PHA Synthesis." Biopolymers 3 (2001).

Sato, Noburu, Laurent Meijer, Leandros Skaltsounis, Paul Greengard, and Ali H. Brivanlou. "Maintenance of Pluripotency in Human and Mouse Embryonic Stem Cells Through Activation of Wnt Signaling by a by a Pharmacological Gsk-3-Specific Inhibitor." Nature Medicine 10 (2005): 55-63.

Shlegel, H, and G. Gottschalk. "Formation and Utilization of Poly--Hydroxybutyric Acid by Knallgas Bacteria (Hydrogenomonas)." Nature 191 (1961): 463-465.

Wang, Yongzhong, Hyeon-Joo Kim, Gordana Vunjak-Novakovic, and David L. Kaplan. "Stem Cell-Based Tissue Engineering with Silk Biomaterials." Biomaterials 27 (2006): 6064-6082.

Wobus, Anna M., and Kenneth R. Boheler. "Embryonic Stem Cells: Prospects for Developmental Biology and Cell Therapy." Physiol. Rev. 85 (2005): 635-678.

Xu, Yue, Yan Shi, and Sheng Ding. "A Chemical Approach to Stem-Cell Biology and Regenerative Medicine." Nature 453 (2008): 338-344.

**CHAPTER 2**  
**MESC BIOCOMPATIBILITY ON TWO DIMENSIONAL SOLID SURFACES**  
**MODIFIED WITH PHB VIA ENZYMATIC SURFACE-INITIATED**  
**POLYMERIZATION**

**2.1 Abstract**

The use of embryonic stem cells (ESCs) holds great promise for use in regenerative medicine and tissue engineering, due to their ability to differentiate into derivatives of the three primary germ layers. For such uses, the ESCs must first be propagated in an undifferentiated state. The suitability of using Enzymatic Surface-Initiated Polymerization (ESIP) of polyhydroxybutyrate (PHB) on gold surfaces was evaluated to determine proliferation of murine ESCs in an undifferentiated state.

Three surfaces were compared with respect to gold alone: ESIP Au/PHB, ESIP Au/PHB-BSA, and compression molded PHB (PHB<sub>cm</sub>). Tissue culture polystyrene (TCPS) was also used as a reference sample, as this is the conventional surface used for propagation of mESCs. Our results showed that Au/PHB-BSA supported far greater mESC proliferation over a long term period than Au/PHB or Au alone. In comparison to TCPS, ESIP Au/PHB-BSA performed almost as well. These results suggest that ESIP-PHB may be useful for expanding mESCs in an undifferentiated state, a process requisite for their application in tissue engineering.

## **2.2 Introduction**

Embryonic stem cells have the unique properties of self-renewal for an undefined period of time and the capacity to differentiate into all cell types from the three primary germ layers (Keller 2005). Since the isolation of murine embryonic stem cells in 1981 (Evans et. al. 1981, Martin 1981), the potential for using these pluripotent cells in regenerative medicine has been heavily evaluated (Wobus and Boheler 2003). However, in order to differentiate mESCs into adult subtypes for use in various tissue engineering applications, they must first be expanded in an undifferentiated state.

The widely used method for propagating undifferentiated ES cells involves culture upon a feeder layer of mitotically inactivated mouse embryonic fibroblasts (MEFs) along with the addition of leukemia inhibitory factor (LIF) (Nichols et. al. 1990, Williams et. al. 1988). LIF is a cytokine and member of the Interleukin-6 family. By activating the JAK/STAT signaling cascade, it maintains the self-renewing capacity of ES cells (Heinrich et. al. 1998). Without the feeder cells and LIF, the ES cells will undergo spontaneous differentiation to form a heterogeneous population of adult cell subtypes (Çetinkaya et. al. 2007).

In addition to these signaling factors, it has been shown that topographical cues can also affect cell behavior (Dawson et. al. 2008). Recent studies have looked into various surfaces suitable for maintaining undifferentiated ES cells as well as providing a platform for subsequent differentiation once an adequate population size has been reached (Chai and Leong 2007). One such work focused on immobilizing LIF onto polyester fabric substrates for the propagation of ES cells without the need for feeder cells and LIF-supplemented media (Çetinkaya et. al. 2007).



Though this system was capable of maintaining a significant percentage of undifferentiated ES cells, it was not superior to the feeder layer control. Another study evaluated covalently immobilized four different azidophenyl-derivatized polymers (poly (acrylic acid), polyallylamine, poly(2-methacryloyloxyethyl phosphorylcholine-co-methacrylic acid), and gelatin) onto polystyrene tissue culture dishes (Konno et. al. 2006). It was found that azidophenyl-derivatized gelatin surfaces showed the greatest ES cell attachment and colonization, but not to levels greater than that of normal gelatin coated surfaces. Various poly( $\alpha$ -hydroxy ester) surfaces were also evaluated for their ability to support undifferentiated ES cell growth (Harrison et. al. 2004). Treatment of the surfaces with 0.1M KOH to increase hydrophilicity and surface roughness enhanced ES cell colonization, but treatment with 0.4M KOH decreased this effect.

All this research into various biomaterials for stem cell expansion and differentiation collectively shows the importance of evaluating various surfaces for their ability to control stem cell behavior *in vitro*. In this study, the suitability of the enzyme-linked surface initiated polymerization (ESIP) of polyhydroxybutyrate (PHB) as a platform for maintaining and propagating undifferentiated stem cells was evaluated. PHB presents itself as an attractive material for tissue engineering, due to its inherent biocompatibility. It has been shown to enhance proliferation of a variety of cell types including osteoblasts and fibroblasts (Chen et. al. 2003, Niamsiri et. al. 2007, Wu et. al.). Since PHB is amenable to various processing methods, it can be used to create films, fibrous mats, or noncrystalline chains to suit a specific use. Unlike its other variations, ESIP-PHB is formed by immobilizing the PHA synthase enzyme itself onto a surface. Upon addition of the substrate, PHB granular structures form a monolayer upon the surface, with

properties different than the usual compression-molded or meshed PHB. Since the attachment of the PHA synthase can be controlled in a site-specific manner, the PHB granules can be patterned over a surface. Additionally, the inclusion of bovine serum albumin (BSA) during the polymerization significantly increases the formation of these granules (Niamsiri et. al. 2007).

It is envisioned that patterned ESIP-PHB surfaces will allow for patterned ES cell growth, which may not only support for possible undifferentiated expansion, but could permit subsequent differentiation procedures as well. For these future applications, the ability of ESIP-PHB to support undifferentiated ES cell growth must first be evaluated. The objective of this study is to evaluate the ability of ESIP-PHB platforms to support undifferentiated ES cell growth. Four surfaces were studied: gold chips alone (Au), gold chips with ESIP-PHB (Au-PHB), gold chips with ESIP-PHB/BSA (Au-PHB/BSA), and compression-molded PHB (PHB<sub>CM</sub>). As a reference, tissue culture polystyrene was also included as a test surface.

## **2.3 Materials and Methods**

### *Materials*

The following materials were purchased from Sigma-Aldrich (St. Louis, MO) and used as received: DL- $\beta$ -hydroxybutyryl coenzyme A (3HB-CoA), 16-mercaptohexadecanoic acid, trifluoroacetic anhydride, triethylamine, N, N-dimethylformamide, tetrahydrofuran, sodium hydroxide, ethylene-diaminetetraacetic acid, nickel chloride, N, N-bis-(carboxymethyl)-L-lysine-hydrate, triethylene glycol.

### *Bacterial Culture and Enzyme Purification*

Recombinant *Escherichia coli* strain BL21 (DE3) pLysS (Novagen)/pET-C01 was used to produce His<sub>10</sub>-PHA synthase of *Wautersia eutropha* H16 (DSM428) His<sub>10</sub>-PHAC<sub>we</sub>. The purification was similar to documented methods with certain modifications. A 1-l culture with 50 µg/ml ampicillin in Luria-Bertani broth (Bacton, Dickson and Company) was cultured aerobically at 37°C to an optical density of 0.5 measured at 600 nm. Induction of PHA synthase production was performed by adding 200 µM isopropyl-β-D-thiogalactopyranoside (Sigma, St.Louis, MO) to the culture and transferring it to a shaking incubator for an extra 5 hours at 30°C. Cells were then collected by centrifugation and stored until purification at -80°C. The purification of His<sub>10</sub>-tagged PhaC<sub>we</sub> used a Ni-NTA agarose chromatography column (Qiagen, Valencia, CA). To summarize, the frozen cell pellet was resuspended in 50 mM Tris-HCl, 10% (v/v) glycerol, 10 mM imidazole pH 7.5 and sonicated on ice for about 1 min in order to lyse the cells. The lysate was then centrifuged at 10, 000 rpm at 4°C for 30 min. The resulting supernatant was purified via metal chelating column chromatography with Ni-NTA pre-equilibrated with 50 mM Tris-HCl, 10% (v/v) glycerol, 10 mM imidazole at pH 7.5. After loading this supernatant, 50 mM Tris-HCl, 10% (v/v) glycerol, 20 mM imidazole, pH 7.5 was then used to wash the column. Elution of His<sub>10</sub>-tagged PhaC<sub>we</sub> was performed with 0 mM Tris-HCl, 10% (v/v) glycerol, 20 mM imidazole, pH 7.5. As a final step, a Bradford Assay was utilized to quantify the final protein concentration.

#### *Preparation of Planar Gold Surfaces and functionalization with NTA-Ni<sup>2+</sup>*

To make the planar surfaces, a 10 nm chromium adhesion layer was deposited onto a clean pyrex wafer, immediately followed by a 30 nm gold layer using a CHA Mark 50 E-Beam Evaporator (CHA Industries, Fremont, CA). To immobilize the His-tagged PHA synthase, the wafers were

then functionalized with NTA-Ni<sup>2+</sup>, using a previously established method (Yan et. al., 1997, Niamsiri et. al., 2007). Briefly, the wafers were immersed overnight in an ethanolic solution with 2mM 16-mercaptohexadecanoic acid to create a self-assembled monolayer of carboxylic acid. The wafer was then rinsed in ethanol, dried with nitrogen gas, and then immersed in a solution containing 0.1 M trifluoroacetic anhydride and 0.2 M triethylamine in anhydrous N-N-dimethylformamide to create interchain anhydride groups. Afterwards, the wafer was rinsed with DMF, dried with nitrogen gas, and immersed in another solution with 10 mM N, N-bis-(carboxymethyl)-L-lysine-hydrate (AB-NTA), 10 mM triethylene glycol, and 7.5 mM NaOH. This created NTA functional groups and carboxylic acids on the surface. After approximately half an hour of immersion, the surface was rinsed with deionized water and dried with nitrogen gas. The NTA groups were complexed with nickel by immersion of the wafer in a 40 mM NiCl<sub>2</sub> solution for 2 h. The wafers were then rinsed with deionized water, dried under nitrogen gas, and cut into 1 cm x 1 cm chips using a diamond-tipped pen.

#### *Enzymatic Surface-Initiated Polymerization of PHB*

The *in situ* polymerization of PHB was performed in a two-step process: 1) immobilization of the enzyme onto the surface and 2) polymerization of PHB upon addition of the substrate. The immobilization step involved immersing each NTA-Ni<sup>2+</sup> functionalized chip in PBS (pH 7.4) with 200  $\mu$ L purified PHA synthase and incubating it at room temperature for 2 hrs with moderate agitation. For the polymerization step, the chips were immersed in a PBS solution with 50  $\mu$ L of the substrate (3HB-CoA) at room temperature for at least 12 hrs. After polymerization, the chips were dried with a stream of nitrogen gas. For the Au/PHB-BSA chips, 500  $\mu$ L of BSA

[2mg/mL] was added to both the immobilization and polymerization steps. Prior to cell culture, the chips were sterilized for 3 hrs under an ultraviolet light.

### *Cell Culture on Planar Surfaces*

The murine embryonic stem cells were grown on top of a monolayer of mitotically inactivated MEFs in Dulbecco's Modified Eagle's medium (DMEM) supplemented with 15% fetal bovine serum, with 1% of non-essential amino acids, 100X nucleosides, L-Glutamine, and penicillin/streptomycin. 3.5  $\mu$ L of 0.1 mM  $\beta$ -Mercaptoethanol (Sigma M7522) was also added, along with 1mL of LIF (chemicon international – ESGRO cat# ESG1107) at  $5 \times 10^5$  units/mL. After two passages, the cells were seeded onto the chips at a density of  $5 \times 10^4$  cells/chip. Cell culture on the planar surfaces was performed for one week, and media supplemented with LIF was changed every day. Chips were removed for MTT analysis and immunocytochemistry on days 2, 4 and 7.

### *MTT Assay*

The surfaces for testing were moved to new plates and rinsed thoroughly with PBS (pH 7.4). A Vybrant® MTT cell proliferation assay kit (Molecular Probes, Invitrogen, CA) was used to quantify the number of viable cells present on the surfaces. This assay utilizes the reduction of the tetrazolium salt MTT (3-(4, 5-dimethylthazol-2-yl)-2, 5-diphenyl tetrazolium bromide) into a formazan product by the mitochondrial dehydrogenase of viable cells. Briefly, the chips were moved to a new plate and the adherent cells removed with trypsin. The cells were then resuspended in non-phenol red media, and 100  $\mu$ L of the suspension was pipetted into a 96-well assay plate and incubated for 3 hrs at 37°C. After this time, 10  $\mu$ L of the MTT solution

(5mg/mL in PBS) was added to each well and again incubated for 3 hrs at 37°C. Next, 100  $\mu$ L of an SDS solution in 0.01M HCl was added to each well and again incubated at 37 °C overnight. The plate was then read at 570 nm against the blank which consisted of non-phenol red media without cells. The MTT standard curve was created from treated known amounts of cells with the MTT and SDS solutions. The number of viable cells on the chips could then be calculated from this standard curve.

### *Immunocytochemistry*

The ES cells were also fixed and stained with Oct4, a marker of their undifferentiated state at days 2, 4 and 7 in culture. Briefly, the chips were washed with PBS (pH 7.4) and incubated for 15 min in a solution of 3.7% paraformaldehyde in PBS. The chips were then rinsed twice with PBS, followed by two 10 min incubations in a solution of 0.1% Tween-20 in PBS. The chips were washed in PBS again and then incubated in a blocking buffer (5mg/mL BSA in PBS) overnight at 4°C. The chips were then incubated for 3.5 hrs with Oct4 (C-10): sc-5279 mouse monoclonal antibody (1:50 dilution; Santa Cruz Biotechnology, Inc). The chips were then rinsed thrice for 10 min each with wash buffer (1mg/mL BSA), following by a 1.5 hr incubation at 4°C with Hoechst dye (1:1000, Sigma) to visualize cell nuclei. The chips were then rinsed with DI water and imaged under a fluorescent microscope (Nikon Eclipse E400, Japan) with a camera attachment (Nikon Digital Camera DXM 1200, Japan).

## **2.4 Results and Discussion**

### *Surface Characterization*

Gold chips were used in this study due to the relative ease to chemically modify their surfaces. AFM analysis was used to measure the growth of PHB granules on the chip surface, as shown in figure 1.

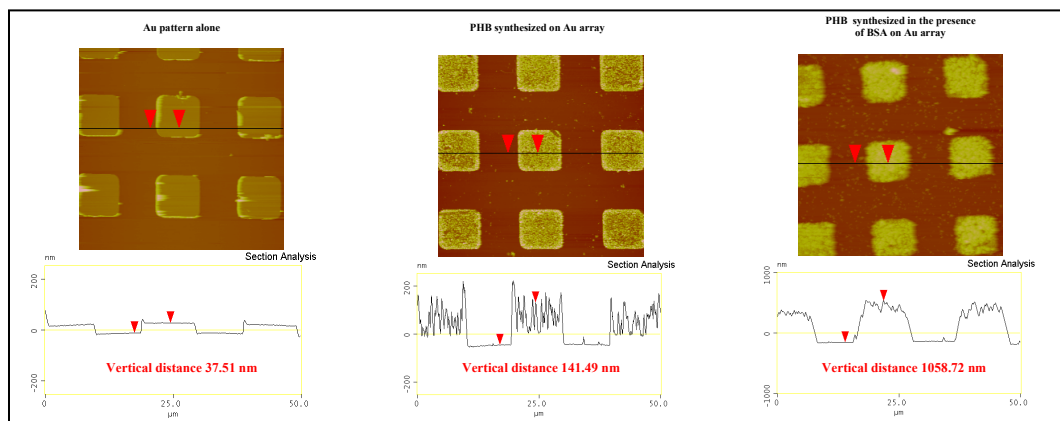


**Figure 1:** AFM analysis of ESIP-PHB on Au arrays shows that ESIP-PHB produces granules with a height of 100 nm. Addition of BSA to the polymerization reaction produces granules with a height of 1000 nm, ten times greater than before. (Niamsiri et. al . 2007)

The growth of the PHB granules was greater on Au/PHB-BSA surfaces. Bovine serum albumin is a hydrophobic plasma protein (McClellan and Frances 2005). As the PHB granules form, the BSA aggregates with it through hydrophobic interactions. This stabilizes the growing polymer, allowing more of the substrate to gain access to the active site of the enzyme, which results in larger granule formation.

### *Cell Proliferation*

On days 2, 4 and 7 of the ES cell culture atop the various surfaces, cells were assessed for their proliferativity and viability. These results are summarized in figure 2.

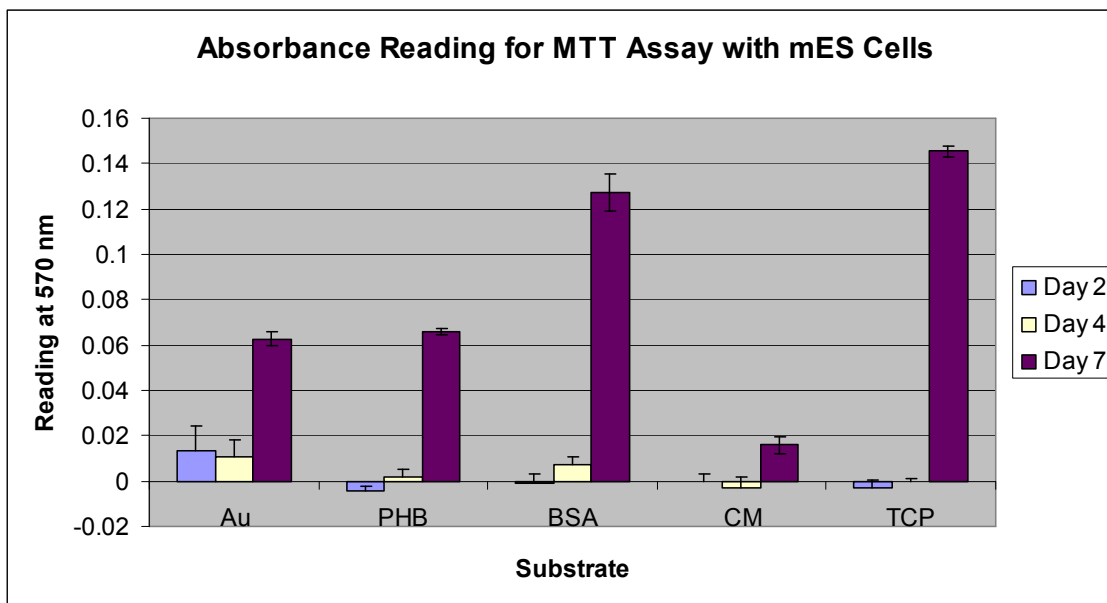


**Figure 2:** Summary of MTT assay for test surfaces.

Conversion of the absorbance readings to cell numbers were performed via use of a standard curve where known amounts of cells were assayed. These results are shown below in figure 3.

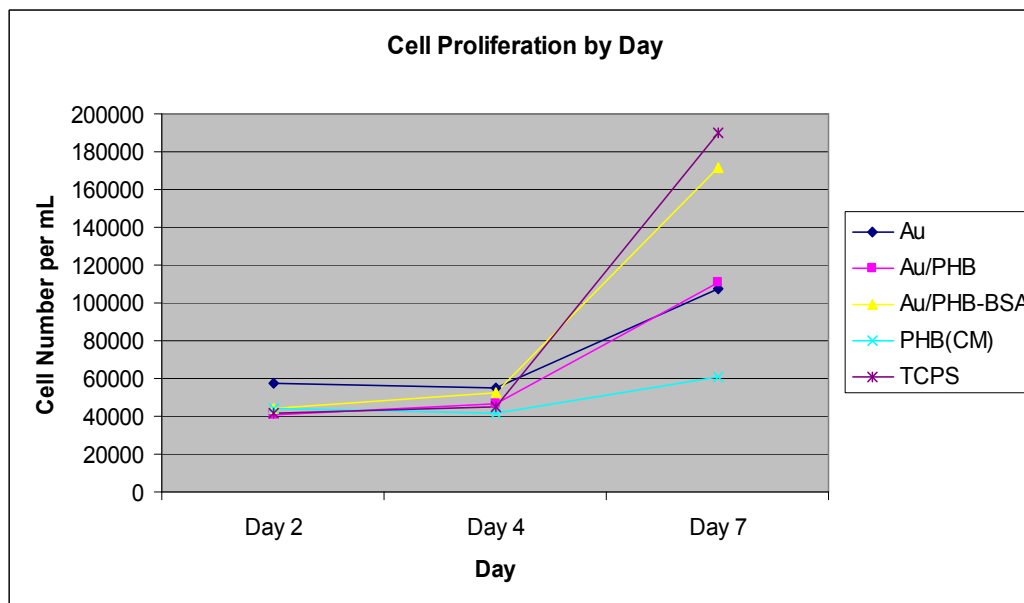


**Figure 3:** Calculation of cell proliferation of test surfaces.



Initially, we found that some of the surfaces would float up slightly, which prevented cells from adhering properly to their surface. This issue resolved itself by day 3 or 4 in culture, which may account for the increased proliferation from days 4 to 7. Additionally, the process of trypsinization and reseeding on the test surfaces may also account for the slowed initial proliferation rates.

While the unmodified gold surfaces supported the greatest initial population of cells, they were unable to support sustained growth. This was true for the PHB<sub>CM</sub> surfaces, which were included as a test surface to show that though the molecular composition may be the same as Au/PHB, it is the surface topography that alters cell behavior. The Au/PHB-BSA surfaces show cell proliferation to a level almost on par with tissue culture polystyrene, and twice the amount of Au/PHB.

### *Immunostaining*

As a qualitative assessment of the undifferentiated state, the cells were stained for Oct-4, a widely used marker for such purposes. Figure 4 shows the results of the staining.

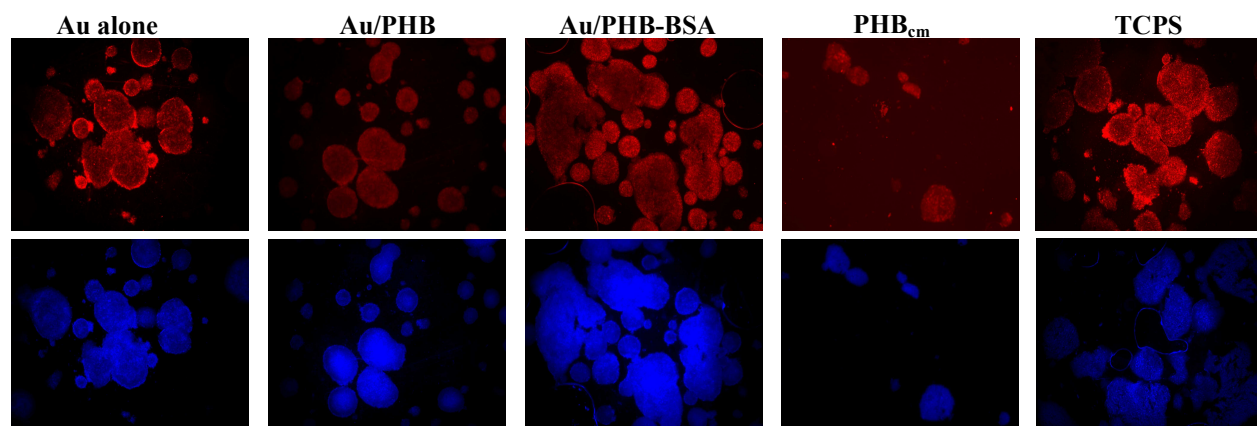


**Figure 4:** Oct 4 (red) and Hoescht (blue) staining for cells after 7 days of culture in the presence of LIF

All the cells remained largely undifferentiated. The quantitative analysis from the MTT assay was supported here, as the largest number of cells was seen on tissue culture polystyrene and Au/PHB-BSA surfaces.

There was some question as to why the Au/PHB-BSA surfaces supported greater cell growth than Au/PHB surfaces. BSA is often used to prevent nonspecific protein adsorption, which would thus decrease cell attachment. Previous studies with patterned ESIP PHB surfaces found that Au/PHB-BSA surfaces supported *less* cell growth than Au/PHB surfaces (Niamsiri 2007). However, ES cells show a very different expression profile than any other adult cells such as MEFs, and have unique properties in culture. They have no quiescent or senescent state, and can still multiply in the absence of serum. Most importantly, they show no contact inhibition or anchorage dependence, as do MEFs (Wobus and Boehler 2005). Because of these properties, it seems as though the PHB granule size plays more of an influence on the ES cell attachment and propagation, which may explain why the ES cells proliferate to a greater extent on the Au/PHB-BSA surfaces.

## **2.5 Conclusions and Future Work**

This work shows that ESIP PHB can support the growth of mouse embryonic stem cells in an undifferentiated state at a level comparable to the widely-used tissue culture polystyrene. Unlike tissue culture polystyrene, ESIP PHB can be patterned, which lends itself to a variety of applications for differentiation purposes. Future work would involve testing the attachment of these cells on patterned surfaces. Since PHB surfaces are biocompatible, it is desired to verify

that mESCs will *preferentially* attach and proliferate on the Au/PHB-BSA surfaces. If this is the case, we envision that ESIP Au/PHB-BSA can be used as a differentiation surface to promote and support the differentiation of embryonic stem cells into neurogenic cells\*. The preferential attachment can be utilized as a technique to pattern the differentiation and growth of the neurogenic cells. This presents useful application in neural tissue engineering, which has promise as therapy for a variety of ailments such a stroke and Parkinson's disease.

## Acknowledgements

I thank Dr. Nuttawee Niamsiri for her surface characterization data and images.

## 2.6 References

Çetinkaya, Gaye, Hilal Türkoğlu, Sezen Arat, Hande Odaman, Mehmet A. Onur, Menemşe Gümüşderelioğlu, and Aşkin Tümer. "LIF-Immobilized Nonwoven Polyester Fabrics for Cultivation of Murine Embryonic Stem Cells." Journal of Biomedical Materials Research Part A 81A (2007): 911-919.

Chai, Chou, and Kam W. Leong. "Biomaterials Approach to Expand and Direct Differentiation of Stem Cells." Molecular Therapy 15 (2007): 467-480.

Dawson, Eileen, Gazell Mapili, Kathryn Erickson, Sabia Taqvi, and Krishnendu Roy. "Biomaterials for Stem Cell Differentiation." Advanced Drug Delivery Reviews 60 (2008): 215-228.

Evans, M J., and M H. Kaufman. "Establishment in Culture of Pluripotential Cells From Mouse Embryos." Nature 292 (1981): 154-156.

Harrison, J, J S. Forsythe, K A. Gross, D R. Nisbet, H Beh, T F. Scott, A O. Trounson, and R Mollard. "Colonization and Maintenance of Murine Embryonic Stem Cells on Poly( $\alpha$ -Hydroxy Esters)." Biomaterials 25 (2004): 4963-4970.

Heinrich, Peter C., Iris Behrmann, Gerhard Muller-Newen, Fred Schaper, and Lutz Graeve. "Interleukin-6-Type Cytokine Signalling Through the Gp130/Jak/STAT Pathway." Biochem. J. 334 (1998): 297-314.

---

\* In order to determine the optimal neurogenic differentiation methodology, we assessed the effects of EB formation on differentiation efficiency. This is addressed in Appendix A.

Keller, Gordon. "Embryonic Stem Cell Differentiation: Emergence of a New Era in Biology and Medicine." Genes and Development 19 (2005): 1129-1155.

Konno, Tomohiro, Naoki Kawazoe, Guoping Chen, and Yoshihiro Ito. "Culture of Mouse Embryonic Stem Cells on Photoimmobilized Polymers." Journal of Bioscience and Bioengineering 102 (2006): 304-310.

Martin, Gail R. "Isolation of a Pluripotent Cell Line From Early Mouse Embryos Cultured in Medium Conditioned by Teratocarcinoma Cells." Proceedings of the National Academy of Sciences 78 (1981): 7634-7638.

McClellan, Scott J., and Elias I. Franses. "Adsorption of Bovine Serum Albumin At Solid/Aqueous Interfaces." Colloids and Surfaces a: Physicochemical and Engineering Aspects 260 (2005): 265-275.

Niamsiri, Nuttawee. Polyhydroxyalkanoates, Biodegradable Polymers From Bacteria: Aspects of Protein Engineering and Applications in Nanobiotechnology and Biomedicine. Diss. Cornell Univ., 2007. Ithaca, 2007.

Nichols, J, Ep Evans, and Ag Smith. "Establishment of Germ-Line-Competent Embryonic Stem (ES) Cells Using Differentiation Inhibiting Activity." Development 110 (1990): 1341-1348.

Williams, RL, DJ Hilton, S Pease, TA illson, CL Stewart, DP Gearing, EF Wagner, Metcalf D, NA Nicola, and NM Gough. "Myeloid Leukaemia Inhibitory Factor Maintains the Developmental Potential of Embryonic Stem Cells." Nature 336 (1988): 684-687.

Wobus, Anna M., and Kenneth R. Boheler. "Embryonic Stem Cells: Prospects for Developmental Biology and Cell Therapy." Physiol. Rev. 85 (2005): 635-678.

# **CHAPTER 3**

## **EVALUATION OF IRON OXIDE NANOPARTICLE – PHA SYNTHASE CONJUGUGATES FOR APPLICATION AS A NONINVASIVE MEANS OF BONE REPAIR**

### **3. 1 Abstract**

Current research for treatment of bone defects includes a particular focus on noninvasive means to encourage osteoblast migration and bone repair. To this end, magnetic iron oxide nanoparticles have been conjugated to the enzyme PHA synthase. Upon injection to the defect site, the conjugates can be held to a specific location via application of a magnet, and create a matrix that allows for osteoblast migration. In this study, the biocompatibility of the nanoparticle-enzyme complex has been assessed in a tissue mimetic setting. The presence of magnetic nanoparticles did not affect osteoblastic cell proliferation or phenotype as measured by an MTT and ALP assay, respectively.

### **3.2 Introduction**

There are 6.3 million fractures that occur annually in the United States, and about 1 million of them require hospitalization (Mistry and Mikos, 2005). Since the severity of these defects varies considerably, there is a correspondingly large range of research into alternative therapeutics. For severe defects, the most commonly used treatment involves autogenic or allogenic grafting of bone. However, this method presents its own set of drawbacks including donor site morbidity and lack of enough material. The ability to provide a noninvasive means to enhance bone regeneration is thus a valuable one.

Several recent studies in bone repair have focused on providing scaffolds that enhance osteogenesis. Gelatin sponges, commercially available as GelFoam® are a promising material due to their biocompatibility, degradability, and flexibility. Osteoblasts seeded onto such scaffolds showed continued growth, but the scaffold itself does not possess adequate mechanical strength for implantation into load-bearing areas of the body (Rohanizadeh et. al. 2006). Bioceramics, composed of hydroxyapatite and/or tricalcium phosphate, are popular due to their integrative nature with native bone tissue and their osteoconductiveness (Cancedda et. al. 2003). However, these materials are somewhat brittle and also prone to fracture upon exposure to higher mechanical forces (Moore et. al. 1987, Grundel et, al. 1991). Coral, a naturally occurring ceramic, possesses an open porosity and mechanical strength ideal for use in bone repair. One study utilized coral exoskeleton in larger bony defects and found that implanted coral vascularized and replaced with newly formed bone (Petite et. al. 2000).

Newer materials, such as carbon nanotubes, have also found application in bone tissue repair.

One group has utilized carbon nanotubes and combined them with PHB and Bioglass® to create a conducting material that also allows for proper mineralization. The advantage to such an electrically conducting scaffold is the potential to monitor and control the *in situ* degradation rate of the material (Misra et. al. 2006). However, the issue with this and the previously mentioned scaffolds is their required implantation, which increases morbidity at the affected site.

To bypass the need for invasive procedures, a magnetic nanoparticle-PHA synthase complex has been developed. This system can be injected at the site of the defect, and held in place by external application of a magnet. After subsequent injection of the substrate, PHB granules will form *in situ* and provide a suitable matrix for osteoblast migration, proliferation, and deposition of hydroxyapatite, the inorganic component of bone. This process is diagrammed in figure 1.

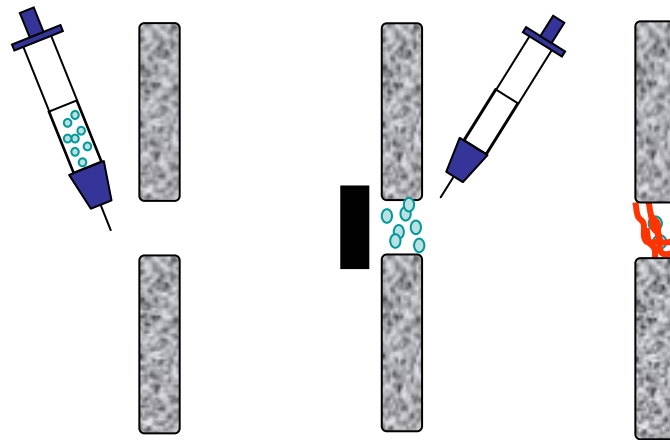


**Figure 1:** Overview of proposed mechanism. Conjugates can be injected to the site of a bone defect and positioned there with a magnet. Upon injection of the substrate, a PHB granule matrix (red) will form, providing a means for osteoblast migration and bone repair.

The focus of this study was to evaluate whether the conjugation of PHA synthase to the nanoparticle affects its polymerization. The directional magnetic control of the conjugates was verified, and any possible negative effects on osteoblastic behavior in a tissue-like setting were investigated.

### **3.3 Materials and Methods**

#### *Materials*

Collacote® strips were obtained from Zimmer Dental. The following materials were purchased from Sigma-Aldrich (St. Louis, MO) and used as received: magnesium chloride, Triton-X100, Tris buffer base.

#### *Nanoparticle Synthesis*

Synthesis of magnetic nanoparticles of 5 nm is diameter was achieved with a previously established method (Sun and Zheng, 2002). Briefly, Fe(acac)<sub>3</sub> ( 2mmol) was mixed in phenyl ether along with 1,2 hexadecanediol (10 mmol), oleic acid (6 mmol), and oleylamine ( 6 mmol) under nitrogen. This resulting mixture was then heated to 250°C at a rate of 4°C/min and refluxed for 30 min. After being allows to cool to room temperature, the dark-brown magnetic nanocrystals were purified by the addition of excess ethanol. Characterization was performed by standard techniques, such as TEM.

#### *Purification of PHA synthase*

Recombinant *Escherichia coli* strain BL21 (DE3) pLysS (Novagen)/pET-C01 was used to produce His<sub>10</sub>-PHA synthase of *Wautersia eutropha* H16 (DSM428) His<sub>10</sub>-PHAC<sub>we</sub>. The purification was similar to documented methods with certain modifications. A 1-l culture with



50 µg/ml ampicillin in Luria-Bertani broth (Bacton, Dickson and Company) was cultured aerobically at 37°C to an optical density of 0.5 measured at 600 nm. Induction of PHA synthase production was performed by adding 200 µM isopropyl-β-D-thiogalactopyranoside (Sigma, St.Louis, MO) to the culture and transferring it to a shaking incubator for an extra 5 hours at 30°C. Cells were then collected by centrifugation and stored until purification at -80°C. The purification of His<sub>10</sub>-tagged PhaC<sub>we</sub> used a Ni-NTA agarose chromatography column (Qiagen, Valencia, CA). To summarize, the frozen cell pellet was resuspended in 50 mM Tris-HCl, 10% (v/v) glycerol, 10 mM imidazole pH 7.5 and sonicated on ice for about 1 min in order to lyse the cells. The lysate was then centrifuged at 10,000 rpm at 4°C for 30 min. The resulting supernatant was purified via metal chelating column chromatography with Ni-NTA pre-equilibrated with 50 mM Tris-HCl, 10% (v/v) glycerol, 10 mM imidazole at pH 7.5. After loading this supernatant, 50 mM Tris-HCl, 10% (v/v) glycerol, 20 mM imidazole, pH 7.5 was then used to wash the column. Elution of His<sub>10</sub>-tagged PhaC<sub>we</sub> was performed with 0 mM Tris-HCl, 10% (v/v) glycerol, 20 mM imidazole, pH 7.5. As a final step, a Bradford Assay was utilized to quantify the final protein concentration.

#### *Conjugating Nanoparticles with PHA Synthase*

The synthesized magnetic nanoparticles are capped with oleic acid, which render the particles hydrophobic. Carboxy-terminated poly (ethylene glycol) molecules are then attached which allows the particles to be suspended in water. The –COOH ends are then converted to NHS esters by mixing the particles with EDC (14mg) and NHS (3.17mg) in a 0.1M MES Buffer (pH 4.5). This was allowed to react for 30 min. The excess reagents were then separated from the particles via size exclusion chromatography. To conjugate the enzyme onto the nanoparticles, in 50mM Phosphate Buffer (pH 7.5) a 1:10 molar ratio of MNP-PL-PEG-NHS-Ester to PHA

Synthase was combined and allowed to react for 2 hrs. The excess enzyme was then removed from the conjugated particles via size exclusion chromatography.

#### *Seeding of the Soas-2 Osteoblastic Cells*

The Collacote strips were cut into 0.5 cm<sup>2</sup> pieces, and UV-sterilized. Afterwards, the scaffolds were hydrated in phosphate buffered saline (pH 7.4). The Soas-2 cells were grown to confluency in two 175 cm<sup>2</sup> flasks in an incubator with 5% CO<sub>2</sub> and at 37°C. At confluence, the cells were removed from the flask using 0.25% trypsin EDTA, and seeded onto the hydrated scaffold at a density of 2 x 10<sup>5</sup>/scaffold. The media was changed every other day. The media consisted of Dulbecco's Modified Eagle's Medium (DMEM) supplemented with 10% fetal bovine serum (FBS) and 1 % pen/strep. The cells were cultured on the scaffold for one week, with assay time points at 2, 4 and 7 days.

#### *MTT Assay*

The scaffolds were transferred to a new plate, and rinsed with PBS (pH 7.4). A Vybrant® MTT cell proliferation assay kit (Molecular Probes, Invitrogen, CA) was used to quantitatively determine the number of viable cells in each scaffold. Briefly, the scaffold were washed twice in PBS (pH 7.4) for 5 min each. Afterwards, 100 µL of trypsin was dripped over the scaffold, and it was incubated for 5 min at 37°C. Non-phenol red media was used to inactivate the trypsin, and pipetted vigorously to remove all the cells from the scaffold. This was then centrifuged at 1000rpm for 5 min. The media was removed, and the cells were resuspended in 500 µL of non-phenol red media and pipetted thoroughly to obtain a homogenous cell suspension. 100 µL of this solution was pipetting into a 96 well clear bottom assay plate, with four replicates for each scaffold. This was allowed to incubate for 3 hrs at 37°C, after which 10 µL of M. This was allowed to incubate for another 3 hrs, after which 100 µL of an SDS solution

in 0.01M HCl was added to dissolve the formazan crystals. After an overnight incubation, the plate was read at 570 nm.

#### *Alkaline Phosphatase (ALP) Assay*

ALP is an enzyme involved in the mineralization, and a marker of proper osteoblastic phenotype. The scaffold was removed and washed twice in PBS (pH 7.4) for 5 min each. Afterwards, 100  $\mu$ L of trypsin was dripped over the scaffold, and it was incubated for 5 min at 37°C. Non-phenol red media was used to inactivate the trypsin, and pipetted vigorously to remove all the cells from the scaffold. This was then centrifuged at 1000rpm for 5 min. The media was removed, and the cells were resuspended in 500  $\mu$ L of lysis buffer (10mM Tris HCl, 2mM  $MgCl_2$ , 0.1% Triton-X100, pH 10). This was put through 3 freeze/thaw cycles to lyse the cells. Each cycle consisted of 20 min freeze time at -80°C followed by 30 min of thawing at room temperature. Next, 100  $\mu$ L of the lysate was mixed with 100  $\mu$ L of p-nitrophenol solution and incubated at 37°C for 30 minutes. The reaction was stopped with 20  $\mu$ L of 1 M NaOH, and read immediately at 410 nm.

#### *Statistical Analysis*

The data analysis tool on Microsoft® Excel was used to perform statistical analyses, including the student's *t* test to assess statistically significant differences.

### **3.4 Results and Discussion**

#### *Assessment of enzyme activity in the conjugates*

To ensure that the conjugation of the enzyme to the nanoparticle did not affect its activity. The PHA synthase substrate was added to a solution containing the conjugates along with Nile Red. Nile red is a lipophilic dye that has an affinity for the hydrophobic PHB granules. The results of an overnight incubation are shown in figure 2.

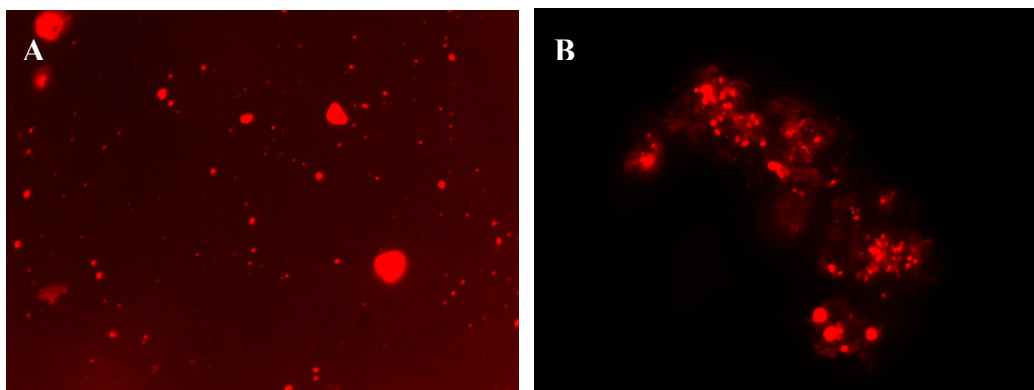


**Figure 2:** Fluorescent images of PHB polymerization by A) PHA synthase alone as well as B) nanoparticle-PHA synthase conjugates

The images seem to suggest that the nanoparticle-PHA synthase conjugates aggregate upon formation of PHB.

Further analysis involved using the TEM, as shown in figure 3.

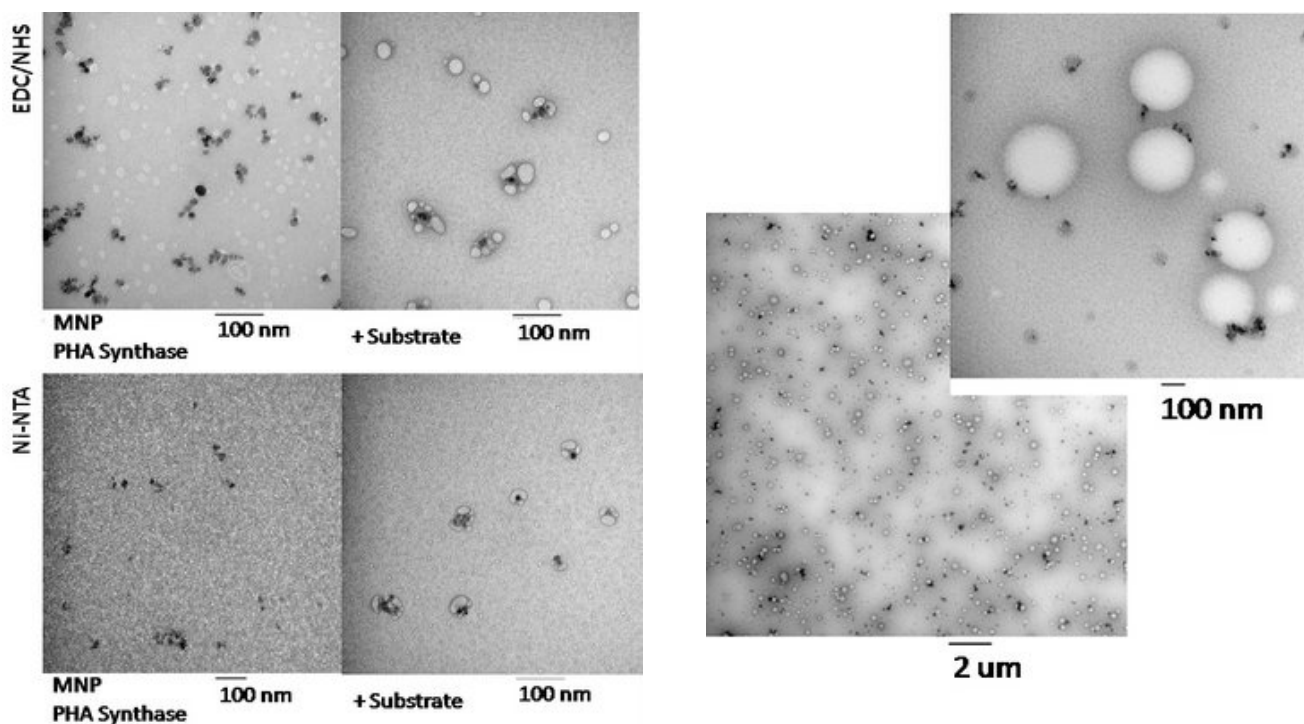


**Figure 3:** TEM analysis of NP-PHA synthase conjugates after overnight polymerization

The PHB granules formed at the nanoparticle surface. It seemed that once the granules grew large enough, they associated with other PHB granules to form aggregates, which correlates with what was seen with the Nile Red images. Collectively, this set of analyses show that PHA synthase activity was maintained and not altered by the conjugation process.

#### *Sensitivity of conjugates to external magnetic control*

Once the activity of the PHA synthase was verified, the magnetic sensitivity of the nanoparticles needed to be ascertained. An initial test involved making 0.5% agarose gels containing the conjugates. After application of an external magnet, the conjugates moved and localized to the area of application, as shown in figure 4.

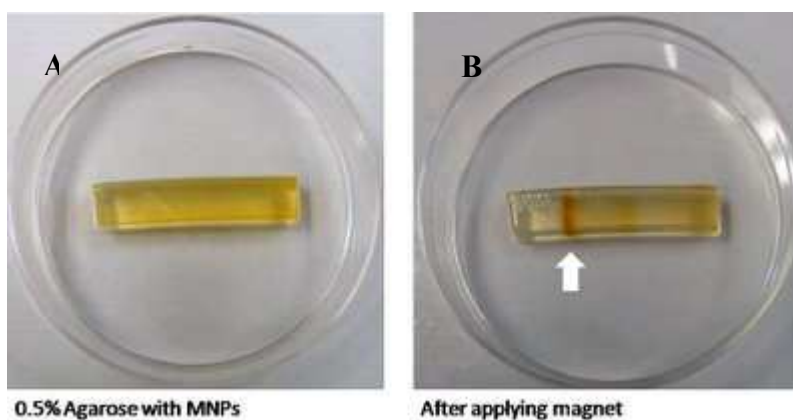


**Figure 4:** Magnetic nanoparticles dispersed throughout an agarose gel (A) will move to a magnetically targeted area (B).

Next, bone samples were acquired from a three day old calf. These were immersed in a solution of conjugates and a magnet was applied to one side of the bone section. After subsequent substrate addition and Nile Red staining, magnetic-localization of the conjugates and polymerization could be ascertained, as shown in figure 5.

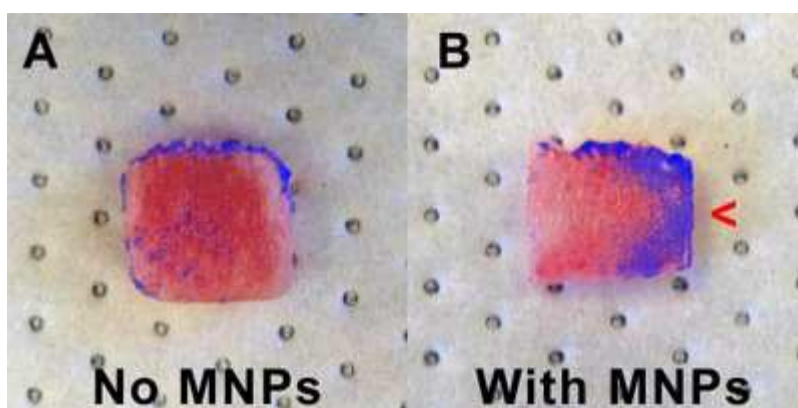


**Figure 5:** A) An untreated section stained with Nile Red. B) A section immersed in conjugates, exposed to a magnet (red arrow) and stained with Nile Red.

#### *Biocompatibility of conjugates with osteoblast-like cells*

In order to be used for bone repair, the compatibility of the nanoparticle system with osteoblasts needs to be assessed first. CollaCote, a commercially available collagen matrix, was used to provide a tissue mimetic scaffold for the biocompatibility study. The cells were seeded onto either unmodified scaffolds, or scaffolds incubated overnight with the conjugate and substrate to allow PHB granule formation throughout the scaffold.

At days 2, 4, and 7 of culture, the scaffolds were assessed for any differences in osteoblast viability and phenotypic changes. A summary of the MTT assay to determine cell viability is shown in figure 6. No significant differences were seen in cell viability.

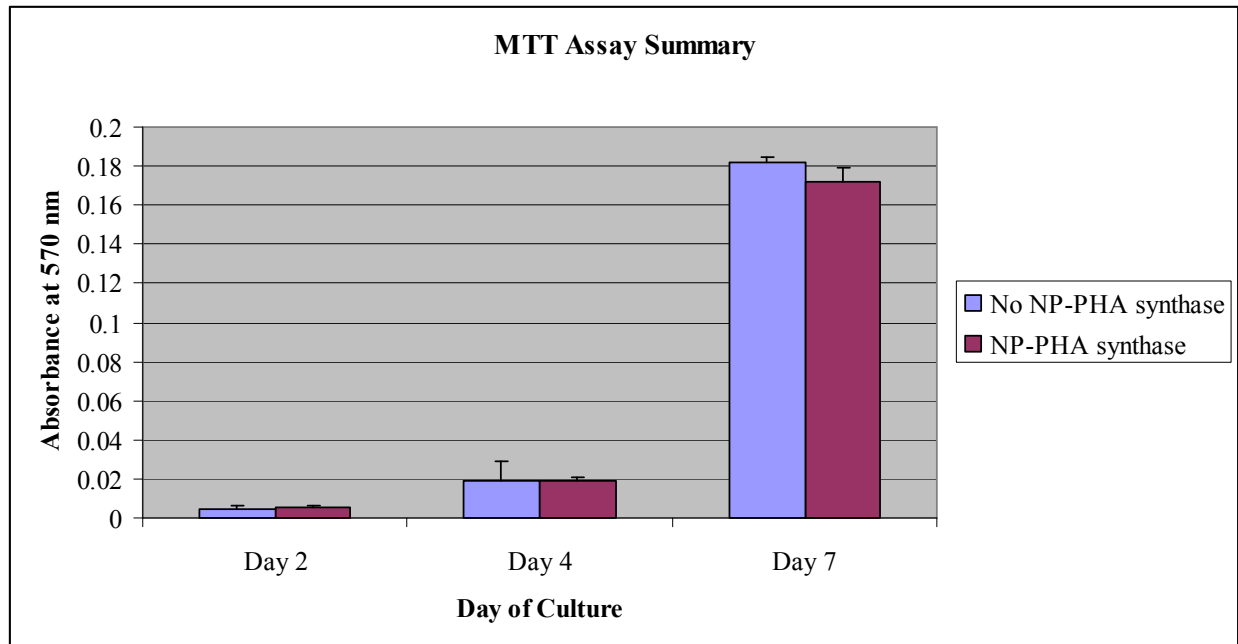


**Figure 6:** MTT Assay Summary for scaffolds with and without conjugate treatment.

To ensure that the conjugates did not alter osteoblast phenotype in any way, an ALP assay was used to quantify any effects. The results of which are summarized in figure 7. ALP activity is responsible for the hydrolysis of substrates containing phosphates, the production of orthophosphate, and the increase in calcium phosphate deposition (Açil et. al. 2000). It has also been linked to the mineralization of collagen sheets (Piattelli et. al. 1996). ALP activity remained fairly constant over the week in culture, again with no significant differences per day between conjugate treated and untreated scaffolds.

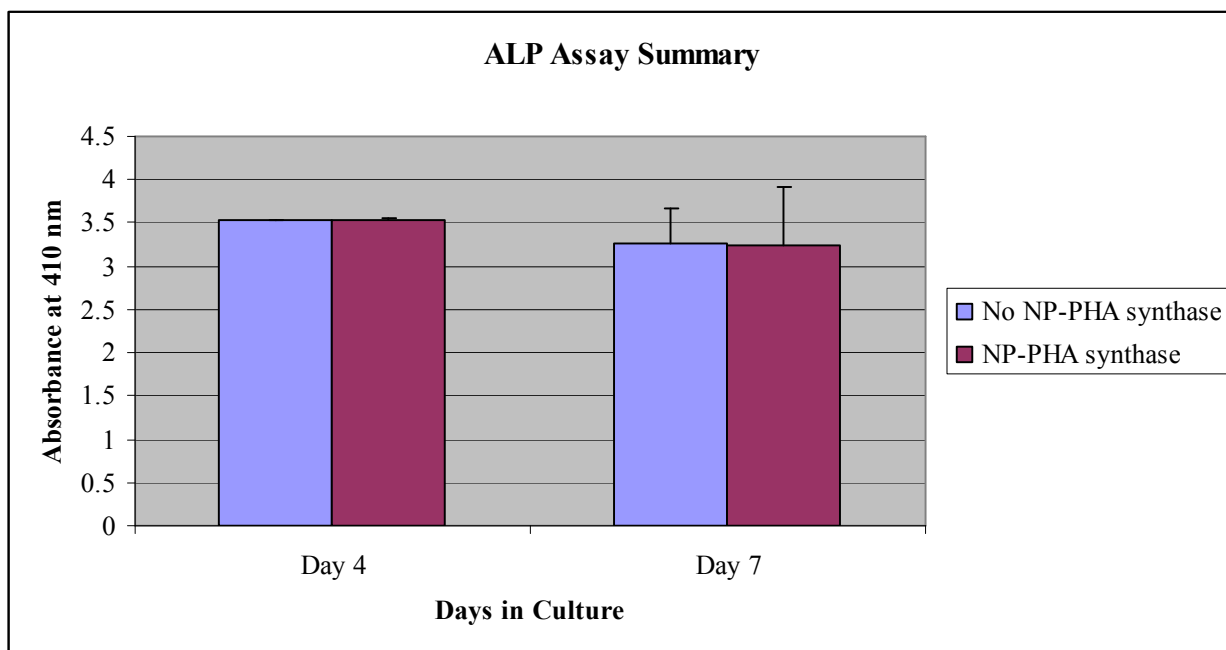


**Figure 7:** ALP Assay Summary for scaffolds with and without conjugate treatment.

Collectively, both assays show that the conjugates do not affect osteoblastic viability or phenotype in a detrimental manner. From the assessment thus far, these conjugates appear promising as a therapeutic to promote osteoblast proliferation and mineralization.

### 3.5 Conclusions and Future Directions

The next step in this study would entail visualization of cell localization within the scaffold itself, once immersed in the conjugate solution and exposed to a magnet. Experiments are underway where the scaffolds have been dispersed with conjugate-formed PHB in a specified area and then seeded with cells. These surfaces will be fixed and then stained to visualize actin filaments, cell nuclei, and PHB granules for observation. To assess any changes in osteoblast mineralization, cells have been seeded on surfaces polymerized with PHB, and additives requisite for mineralization (ascorbic acid,  $\beta$ -glycerophosphate, and dexamethasone) have been



added to the media. After 10 and 14 days, alizarin red and tetracycline pulsing will be used to assess mineralization.

## **Acknowledgements**

I thank Dickson Kirui for his nanoparticles, and Diego Rey for his TEM, agarose, and bone images.

## **References**

Açil, Yahya, Hendrik Terheyden, Anton Dunsche, Bernd Fleiner, and Søren Jepsen. "Three-Dimensional Cultivation of Human Osteoblast-Like Cells on Highly Porous Natural Bone Mineral." Journal of Biomedical Materials Research 51 (2000): 703-710.

Cancedda, Ranieri, Beatrice Dozina, Paolo Giannonia, and Rodolfo Quarto. "Tissue Engineering and Cell Therapy of Cartilage and Bone." Matrix Biology 22 (2003): 81-91.

Grundel, R.E., M.W. Chapman, T. Yee, and D. Moore. "Autogeneic bone marrow and porous biphasic calcium phosphate ceramic for segmental bone defects in the canine ulna." Clin. Orthop. 266 (1991): 244-258.

Misra, SK, P Watts, S Valappil, S Silva, I Roy, and AR Boccaccini. "Poly(3-Hydroxybutyrate)/Bioglass® Composite Films Containing Carbon Nanotubes." Nanotechnology 18 (2007).

Mistry, Amit, and Antonios Mikos. "Tissue Engineering Strategies for Bone Regeneration." Adv Biochem Engin/Biotechnol 94 (2005): 1-22.

Moore, D.C., M. Chapman, and D Manske. "The evaluation of a biphasic calcium phosphate ceramic for use in grafting long-bone diaphyseal defects." J. Orthop. Res. 5 (1987): 356-365.

Piattelli, A, A Scarano, M Corigliano, and M Piattelli. "Effects of Alkaline Phosphatase on Bone Healing Around Plasma-Sprayed Titanium Implants: a Pilot Study in Rabbits." Biomaterials 17 (1996): 1443-1449.

Petite, Herve, Veronique Viateau, Wassila Bensaïd, Alain Meunier, Cindy De Pollak, Marianne Bourguignon, Karim Oudina, Laurent Sedel, and Genevieve Guillemain. "Tissue-Engineered Bone Regeneration." Nature 18 (2000): 959-963.

Rohanizadeh, Ramin, Michael V. Swain, and Rebecca S. Mason. "Gelatin Sponges (Gelfoam®) as a Scaffold for Osteoblasts." J Mater Sci: Mater Med (2006).

Sun, Shouheng, and Hao Zeng. "Size-Controlled Synthesis of Magnetite Nanoparticles." J. Am. Chem. Soc 124 (2002): 8204-8205.

**APPENDIX A**

**EFFECT OF EMBRYOID BODY FORMATION METHODOLOGY ON  
DIFFERENTIATION OF MURINE EMBRYONIC STEM CELLS INTO A NEURONAL  
LINEAGE**

**Abstract**

In *in vitro* culture, mouse embryonic stem cells (mES cells) cluster together into multicellular aggregates termed embryoid bodies (EBs). This is one marker of cell pluripotency as well as being an important step in many differentiation protocols. In two dimensional culture, mES cells aggregate in a heterogeneous manner, forming EBs that are not uniform in size. This can be a vital determining factor on differentiation efficiency. The effects of mES cell culture methodology on EB size was determined, and these differences in terms of neural differentiation efficiency was also assessed. It was found that three dimensional culture homogenized EB size and trypsinizing the cells after exposure to the -4/+4 retinoic acid protocol allowed for greater differentiation efficiency.

## Introduction

Unlike their adult stem cell counterparts, embryonic stem cells (ESCs) are pluripotent, and thus capable of forming any cells derived from the three primary germ layers: endoderm, ectoderm, and mesoderm. This pluripotency has long been thought to be a potential treatment method for a variety of conditions from Alzheimer's Disease to diabetes. However, in order to be used for replacement of damaged tissue, ES cells must first be expanded in an undifferentiated state, and then differentiated.

During *in vitro* culture, ES cells aggregate into a spherical mass termed the embryoid body (EB), which is characteristic prior to the induction of differentiation (Lee et. al. 2000, Dang et. al. 2004). The formation of these EBs is an important step to many differentiation procedures, as EB size can play a determining role in differentiation efficiency. These differentiation protocols are many and varied, and none have a perfect differentiation efficiency. Most of these methods involve the following steps: formation of EBs, addition of cytokine agents to induce lineage-specific differentiation, growth of EBs on adherent culture, and lastly assessment of phenotype.

In addition to their therapeutic potential, EBs themselves have a measure of commercial utility as well. In the pharmaceutical industry, small molecule screens are performed to assess the effects of certain chemicals on cells. EBs are a useful aggregate to perform these high-throughput tests on, as they essentially represent one of the initial stages of a developing organism in an *in vitro* model. One work focused on using EBs as an *in vitro* assay system towards antiangiogenic agents, which has applications towards cancer research (Wartenberg et. al. 1998).

Cardiomyocytes formed from EBs were also used to assess and classify various compounds

based on their teratogenic potential by analyzing the morphology of the beating cardiomyocytes (Seiler et. al. 2004). All these studies implemented either a nonadherent or three-dimensional culture system for the formation of the EBs.

Two-dimensional culture does allow EB formation, but these flat, circular aggregates are highly heterogeneous in both size and morphology. Suspension cultures or the hanging drop method are preferred alternatives for the formation of better spherical aggregates. For suspension culture, bacterial-grade polystyrene is often used, as it inhibits cells attachment and thereby promotes spherical EB formation. The hanging drop method uses bacterial-grade polystyrene, where drops of the ES cell solution are pipetted on the lid, which is then inverted over the dish, as shown in figure 1. This mimics a three-dimensional environment and allows for the formation of homogenous EBs.

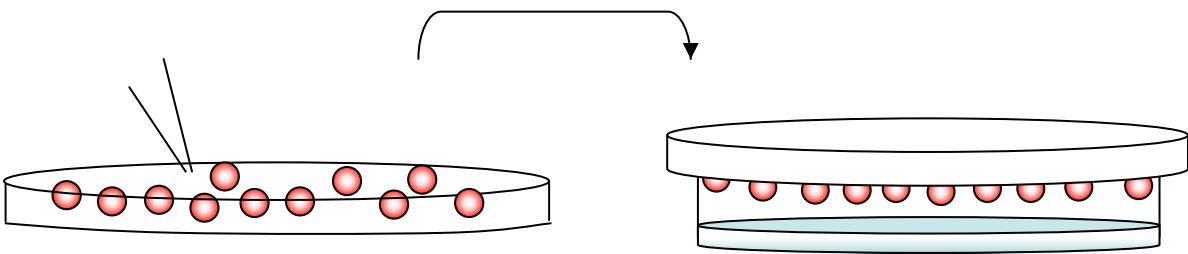


**Figure 1:** Drops of cell solution are pipetted onto the lid of a bacterial Petri dish, and then carefully inverted over a small amount of PBS to create hanging drop culture.

Research into biomaterials for culturing homogenous EBs is ongoing. One group evaluated 2-methacryloyloxyethyl phosphorylcholine (MPC) polymers for their ability to prevent cell adhesion and thus promote spherical EB formation (Konno et. al. 2005). Another group found

that polypropylene conical tubes, easily available in many laboratory settings, provide a simple method for the formation of controlled, homogenous EBs (Kurosawa et. al. 2003).

It was desired to use the patterned ESIP-PHB platform developed in Batt's laboratory to propagate ES cells on a surface, and then direct their differentiation to a neuronal lineage. To this end, the aim of this study was to determine the optimal differentiation procedure based on a combinatorial analysis of the commonly cited methods: nonadherent culture and hanging drop. A non adherent 96 well plate was used as an alternative to the hanging drop method, as it allowed superior control of media and microenvironment conditions.

## **Materials and Methods**

### *ES Cell Culture*

The murine embryonic stem cells were grown on a monolayer of mitotically inactivated MEFs in Dulbecco's Modified Eagle's medium (DMEM) supplemented with 15% fetal bovine serum, with 1% of non-essential amino acids, 100X nucleosides, L-Glutamine, and penicillin/streptomycin. 3.5 µl of 0.1 mM β-Mercaptoethanol (Sigma M7522) was also added, along with 1mL of LIF (chemicon international – ESGRO cat# ESG1107) at  $5 \times 10^5$  units/ml.

### *EB formation and Differentiation into Neuronal Subtypes*

After two passages, the ES cells were trypsinized and seeded onto either nonadherent Petri dishes at a density  $1.75 \times 10^6$  cells or 96 well plates at a density of 5000 cells/well. After 4 days of culture without LIF in either the Petri dishes or 96 well plates, the media was removed and replaced with media containing 1µM all-trans retinoic acid (RA) without LIF. This was

maintained for 4 days, and then the EBs were either left intact or trypsinized before plating onto tissue culture polystyrene.

### *Immunocytochemistry*

After 4 days of culture on the adherent tissue culture polystyrene, the cells were fixed and stained for Oct-4, nestin, and Sox2. To summarize, the cells were washed with PBS (pH 7.4) and incubated for 15 min in a solution of 3.7% paraformaldehyde in PBS. The cells were then rinsed twice with PBS, followed by two 10 min incubations in a solution of 0.1% Tween-20 in PBS. The cells were washed in PBS again and then incubated in a blocking buffer (5mg/mL BSA in PBS) overnight at 4°C. The chips were then incubated for 3.5 hrs with either Oct4, nestin, or Sox2. The chips were then rinsed thrice for 10 min each with wash buffer (1mg/mL BSA), following by a 1.5 hr incubation at 4°C with Hoechst dye (1:1000, Sigma) to visualize cell nuclei. The chips were then rinsed with PBS and imaged under a fluorescent microscope (Nikon Eclipse E400, Japan) with a camera attachment (Nikon Digital Camera DXM 1200, Japan).

## **Results and Discussion**

### *EB formation and differentiation*

The commonly cited differentiation protocols for generating neuronal precursors implement a -4/+4 retinoic acid protocol. After the exposure, the EBs may or may not be dissociated with trypsin and then plated onto an adherent surface. Assessment of these various protocols was necessary to determine which provided the best outcome. The experimental schematic we followed is shown in figure 2.

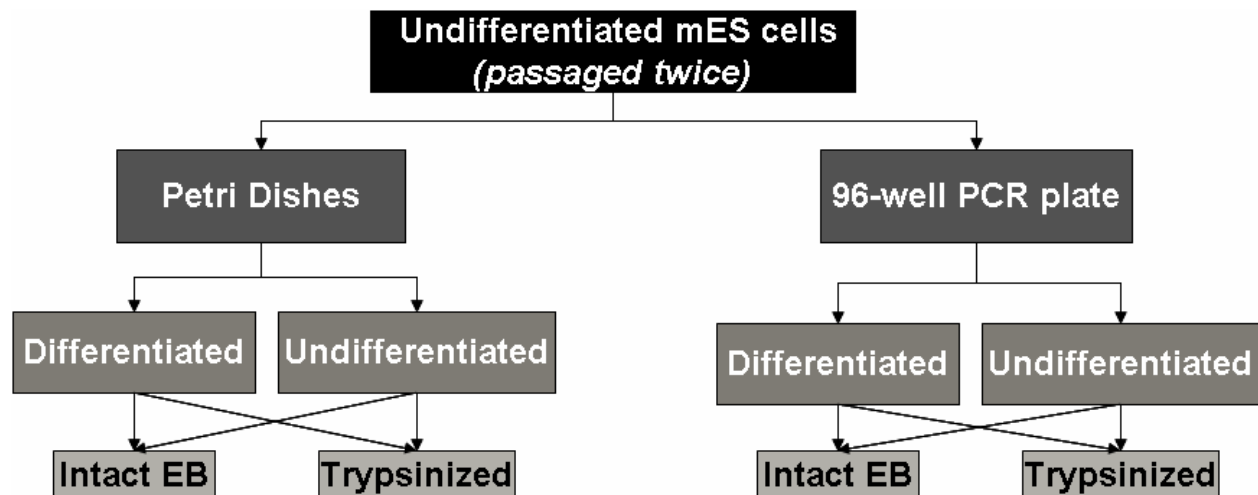


**Figure 2:** Experimental Schematic to determine effects of EB size of differentiation efficiency

Even though the bacterial-grade polystyrene dishes allow for the formation of a large number of spherical aggregates, these are often heterogeneous in size. By placing a specific number in each well of the nonadherent 96-well culture plates, homogenous EBs of a defined cell size were formed, as shown in figure 3. Unlike the hanging drop method, which allows the same control, the media in these wells can be changed or substituted with differentiation media relatively easily.

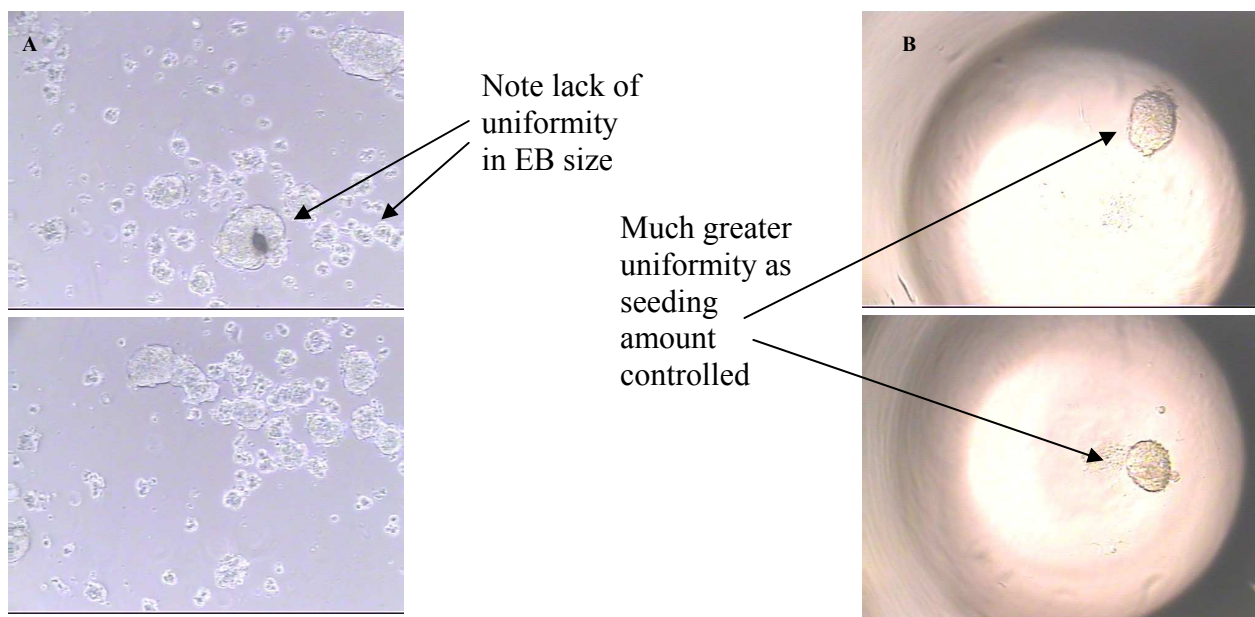




**Figure 3:** Comparison of EB forming methods in bacterial-grade polystyrene (A) to 96 well plates (B) after 1 day in culture. Both cultures are nonadherent.

Both bacterial grade polystyrene and 96 well plates allowed for the formation of spherical EBs, unlike two-dimensional culture on tissue culture polystyrene, which is shown in figure 4.



**Figure 4:** ES cells forming EBs on a flat tissue culture plate. Note the non-uniformity in EB size and shape.

After the -4/+4 induction treatment, we found that treated EBs had greater cell proliferation, and a greater separation of cells was observed around the EBs compared to the untreated cells, as shown in figure 5.

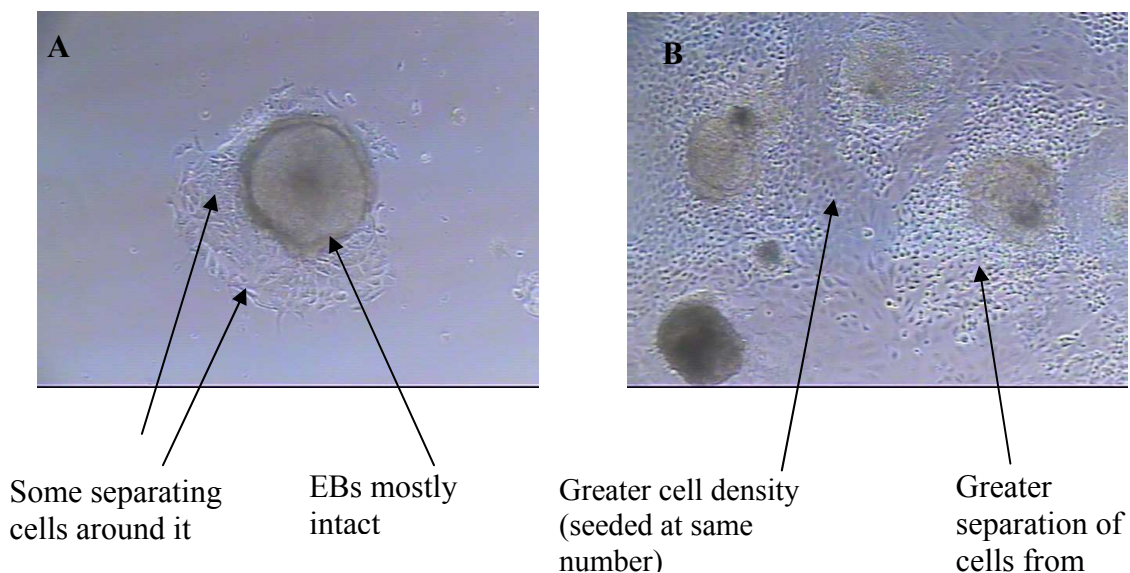


**Figure 5:** Comparison of EB morphology of undifferentiated EB (A) to EBs after exposure to retinoic acid procedure (B). Images are for EBs formed in 96 well plate.

Characteristic morphological changes in the treated cells were observed, such as the formation of neurite outgrowths, as shown in figure 6.

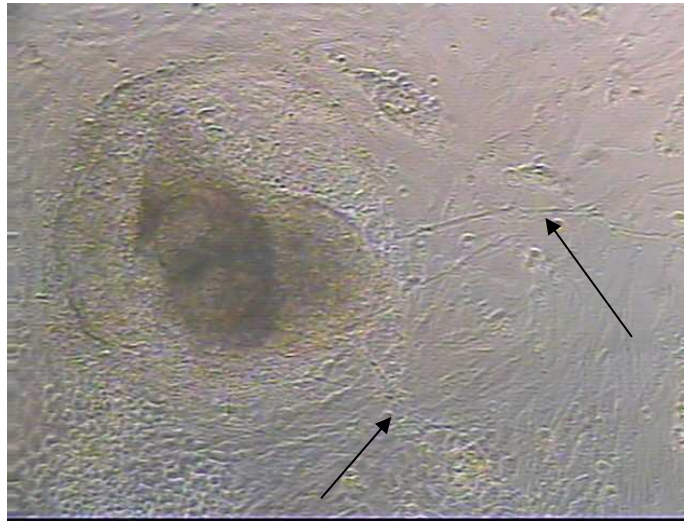


**Figure 6:** Black arrows indicate formation of neurite outgrowth.

Four days after the -4/+4 RA procedure, the cells were further analyzed via immunocytochemistry for Sox2 and nestin. Sox 2 is a marker expressed in neurogenic regions, but its expression declines upon terminal neural differentiation. It is this implicated in maintaining a neural progenitor state. Nestin is an intermediate filament protein primarily expressed during neural development. The results of this staining are shown in figures 7 and 8.

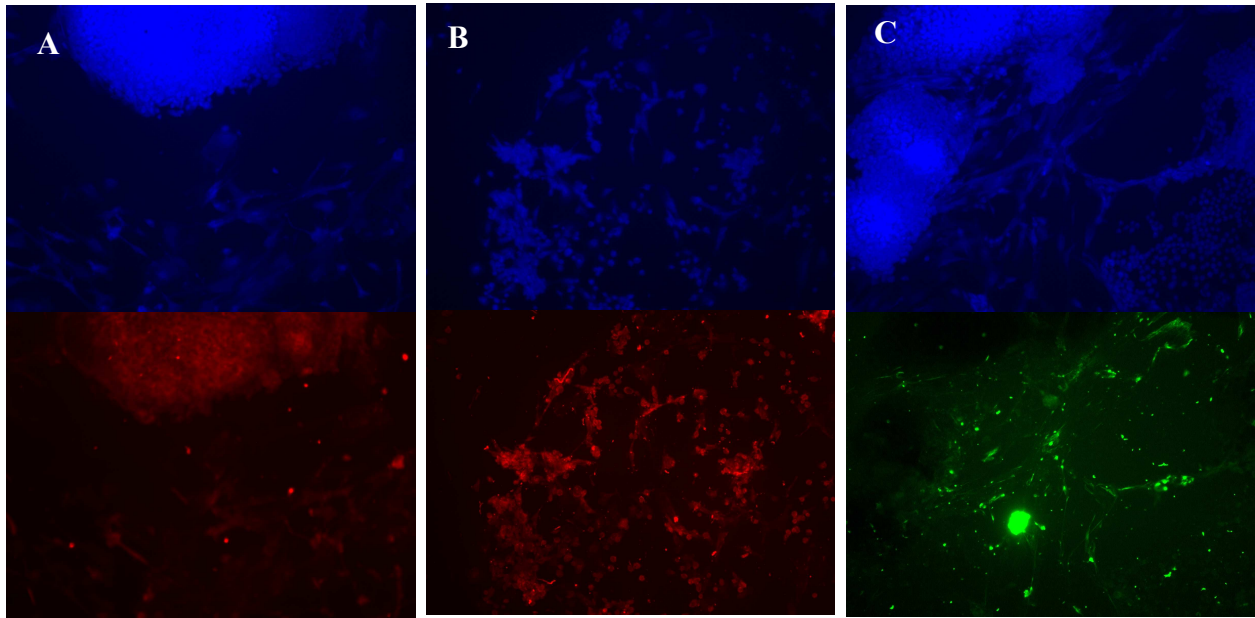


**Figure 7:** Trypsinized EBs from a Petri dish 4 days after the RA treatment. Staining is for A) Oct-4, B) Sox2, and C) nestin.

The expression of Oct4 can still be seen, but when compared to that of the undifferentiated cells, is much less. In contrast, expression of Sox2 is greater in the differentiated cells. Nestin is expressed in both differentiated and undifferentiated cells, but its expression in the RA treated cells was seen throughout the EBs, and not just around its periphery.

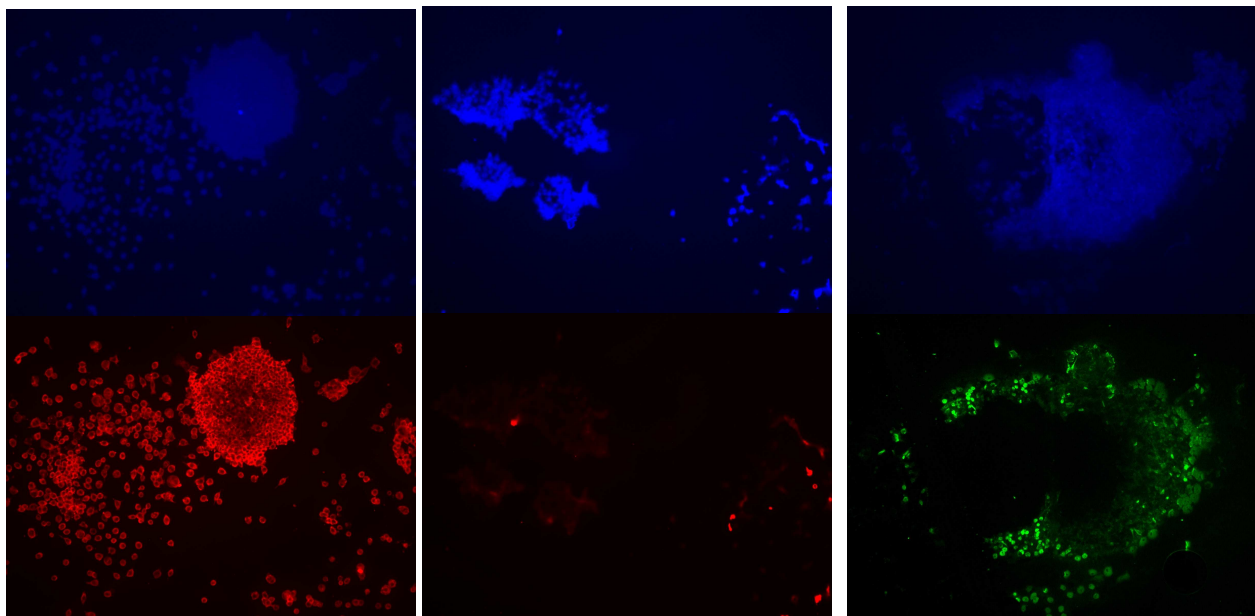


**Figure 8:** Intact undifferentiated EBs from a Petri dish. Staining is for A) Oct-4, B) Sox2, and C) nestin.

Even with LIF supplementation, ES cells show signs of differentiation around the periphery of the EBs, especially with extended time in culture.

## **Conclusion and Future Directions**

With the establishment of a differentiation process with the best degree of efficiency, it can be applied to further our applications with ESIP-PHB. Future work will involve growing ES cells on micropatterned surfaces and qualifying the effects of a patterned surface on differentiation into neural lineages.

## **References**

Dang, SM, S Gerecht-Nir, J Chen, J Itskovitz-Eldor, and Peter W. Zandstra. "Controlled, Scalable Embryonic Stem Cell Differentiation Culture." Stem Cells 22 (2004): 275-282.

Konno, Tomohiro, Kunihiro Akita, Kimio Kurita, and Yoshihiro Ito. "Formation of Embryoid Bodies by Mouse Embryonic Stem Cells on Plastic Surfaces." Journal of Bioscience and Bioengineering 100 (2005): 88-93.

Kurosawa, Hiroshi, Tetsuya Imamura, Mikiko Koike, Katsunori Sasaki, and Yoshifumi Amano. "A Simple Methods for Forming Embryoid Body From Mouse Embryonic Stem Cells." Journal of Bioscience and Bioengineering 96 (2003): 409-411.

Kurosawa, Hiroshi. "Methods for Inducing Embryoid Body Formation: in Vitro Differentiation System of Embryonic Stem Cells." Journal of Bioscience and Bioengineering 103 (2007): 389-398.

Lee, SH, N Lumelsky, L Studer, JM Auerbach, and R McKay. "Efficient Generation of Midbrain and Hindbrain Neurons From Mouse Embryonic Stem Cells." Nature Biotechnology 18 (2000): 675-679.

Seiler, Andrea, Anke Visan, Roland Buesen, Elke Genschow, and Horst Spielmann. "Improvement of an in Vitro Stem Cell Assay for Developmental Toxicity: the Use of Molecular Endpoints in the Embryonic Stem Cell Test." Reproductive Toxicity 18 (2004): 231-240.

Wartenberg, M, J Günther, J Hescheler, and H Sauer. "The Embryoid Body as a Novel in Vitro Assay System for Antiangiogenic Agents." Laboratory Investigation 78 (1998): 1301-1314.